

Non-linear Image-Based Regression of Body Segment Parameters

S.N. Le¹, M.K. Lee^{2,3} and A.C. Fang¹

¹ Department of Computer Science, National University of Singapore, Singapore

² School of Sports, Health and Leisure, Republic Polytechnic, Singapore

³ Physical Education and Sports Science, National Institute of Education, Nanyang Technological University, Singapore

Abstract— Biomechanical analysis of human movement often requires accurate estimation of body segment parameters (BSP). These values are segmental inertial properties, including mass, center of mass and moments of inertia. They can be measured directly on living subjects using techniques such as Magnetic Resonance Imaging (MRI), Computed Tomography (CT) and gamma-mass scanning. Despite their accuracy, these methods involve high radiation and require expensive scanners that are not always readily available to biomechanics researchers. Another popular way to estimate BSP is by studying regression equations on experimental data, commonly from cadaveric studies. These approaches, however, have been criticized for the limited cadaveric data.

We propose a novel in vivo regression method for computing BSP using non-linear image-based techniques. Our method was first facilitated with X-ray images of sample subjects acquired from Dual-energy X-ray Absorptiometry (DXA), where the radiation dose is approximately 1/10th that of a standard chest X-ray. A feature-based image transformation was then applied to predict a mass distribution image for the new subject, while he was not required to undergo DXA scanning. The subject's BSP values were subsequently computed using the mass distribution obtained from the predicted image. Cross-validation of moments of inertia among population samples shows that our method has mean percentage errors of 7.5% for limbs and 7.1% for head and torso, while the corresponding errors are 9.3% and 15% in cadaver-based non-linear regression method. It suggests that our image-based regression approach is promising for estimating BSP on living subjects. It is not limited by ranges of cadaveric data or differences between living and dead tissues.

Keywords— Body Segment Parameters, Dual-energy X-ray Absorptiometry, Image Warping, Regression Method.

I. INTRODUCTION

Body segment parameters (BSP) are the inertial properties of each segment of the anthropometric model, which consist of mass, center of mass and moments of inertia. The accuracy of BSP estimation has a significant influence on mechanical quantities computations, including calculating the kinetics of motion using inverse or forward dynamics [6, 18], gait analysis [16], and determining the sensitivity of joint resultants [1].

Where in vivo methods are unavailable, one popular way to estimate BSP is by constructing statistical models from cadaveric data [4]. [2] and [19] developed regression equations using non-uniform spatial scaling of segmental mass. In other studies, moments of inertia were estimated from segmental measurements [10] or body mass and standing height of the subject [5]. Although cadaver-based methods provide a convenient means to predict BSP, they have been criticized for limited number of samples and variety of sample population. Due to obvious difficulties in acquiring comprehensive cadaveric data, researchers have turned to in vivo methods.

Three-dimensional (3-D) in vivo imaging techniques, such as MRI [14], CT [11, 15] and gamma-mass scanning [20], have been used for determining accurate 3-D BSP. However, they have been criticized for the high level of radiation involved, cost of the scans and limited availability of expensive scanners.

In recent years, two-dimensional (2-D) in vivo imaging techniques using Dual-energy X-ray Absorptiometry (DXA) has been found to be useful for obtaining accurate 2-D BSP [7]. Despite their 2-D nature, the results hold promise as, compared to 3-D imaging, DXA scanning is less expensive while delivering a much lower dose of radiation.

We propose a new approach for estimating a subject's BSP using a feature-based image warping technique facilitated by a set of sample DXA images. Our method predicts a mass distribution image that is statistically representative of the subject by computing a non-linear image transformation based on feature correspondences. To provide the features required in the transformation, each DXA image was annotated with external anthropometric and body segmentation information. Subsequently, BSP values were obtained directly from the predicted mass image. The novelty of our approach is that mass distributions are represented and processed in their raw image form. This is in contrast with previous approaches where regression models are formulated by associating aggregated quantities, such as moments of inertia with external anthropometric. We retain the details in spatial variations of mass, which would have been lost in the aggregated quantities.

In section II, we present our method of estimating BSP from DXA images using non-linear image-based techniques. Section III compares the errors between our computed BSP and that from cadaver-based non-linear regression equations [15]. Section IV presents further discussions and conclusions.

II. MATERIALS AND METHOD

A. Dual-energy X-ray Absorptiometry

DXA machine (QDR-1000/W, Hologic Inc., Bedford, MA, USA) uses two X-ray beams of alternating intensities to measure areal body density (gcm^{-2}) and body composition. The scanning process is done with the help of Hologic QDR Software. The high-energy beam passes through all matter in its path and is attenuated depending on the amount of mass present, which can be illustrated by plotting the attenuations along each scanline of the scanned image. Attenuation values are recorded in rectangular cells of $1.303\text{cm} \times 0.618\text{cm}$ or 150×106 pixels per whole body, resulting in a scan area of $195.5\text{cm} \times 65.5\text{cm}$. Higher attenuation indicates higher mass in each cell (Fig. 1).

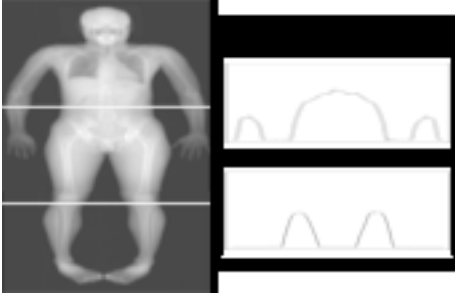


Figure 1: Whole body DXA scan of an adult male subject. Two scanlines crossing belly and knees show attenuation values changing according to the mass present. The raw attenuation image has a resolution of 150×106 .

B. Mass distribution image from DXA

Prior to building mass distribution image, we increased the resolution of DXA attenuation image by applying a bicubic spline interpolation [17]. The process is necessary for an accurate BSP computation. We applied two cubic spline interpolations, one along horizontal direction and one along vertical direction to increase each dimension by 3 times and 5 times respectively. The added pixels' attenuations were interpolated from original pixels' values. The resulting image has a dimension of 750×318 , or $0.2606\text{cm} \times 0.2059\text{cm}$ per pixel.

Each pixel represents the attenuations of the high-energy beam linearly attenuated by the amount of mass present along the beam [7]. The relationship between attenuation and mass can be represented as follows:

$$m(x) = \sigma(a(x)) = m_1 a(x) + m_0 \quad (1)$$

where $m(x)$ and $a(x)$ are the mass (g) and attenuation values respectively at pixel position $x \in R^2$.

We obtained m_1 and m_0 by scanning reams of consumer-grade photocopier paper arranged in five stacks of

increasing height (Fig. 2, Left). The projected region of each stack was determined using a flood-fill algorithm [9] initiated by a mouse click at the approximate center of each region. The mass of each stack was then measured with a weighing scale of precision level up to 0.001kg .

The per-pixel projected mass was calculated by taking the mass of each stack divided by the number of pixels in corresponding region. Similarly, the average per-pixel attenuation in each region was calculated by dividing the sum of the attenuation values by the number of corresponding pixels. In addition, we averaged the background attenuation, which has zero mass, to obtain a total of six mass-versus-attenuation calibration points. The calibration line was used to compute the parameters for Eq. 1.

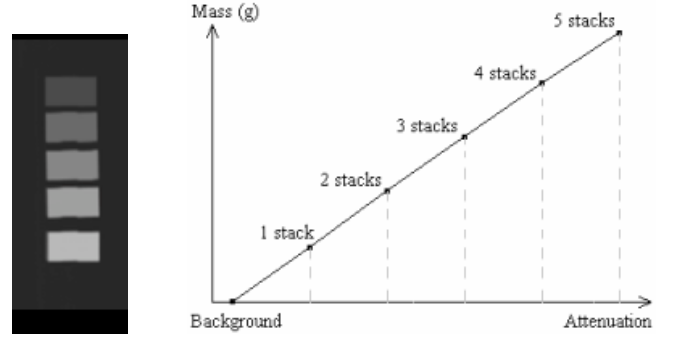


Figure 2: Phantom setup for calibrating the relationship between mass and attenuation. (Left) Scanned image of five stacks of photocopy paper with increasing mass. (Right) Attenuation-to-mass calibration line, which goes through background point and five points representing five stacks.

C. BSP computation using mass distribution image

Whole body image is segmented into 14 parts (Fig. 3). The segmenting lines between limbs cross the bones at joints. We computed BSP for each segment using mass per pixel values obtained directly from mass distribution image.

Mass of each segment k , M_k , was computed by taking the sum of masses at all pixels belonging to that segment:

$$M_k = \sum_{x \in k} m(x) \quad (2)$$

where the attenuation-to-mass conversion (Eq. 1) was used to evaluate each pixel's mass.

Center of mass of segment k , c_k , is computed as follows:

$$c_k = \frac{1}{M_k} \sum_{x \in k} m(x)x \quad (3)$$

Moments of inertia of segment k about the front-to-back axis passing through c_k is calculated as follows:

$$I_k = \sum_{x \in k} m(x) |x - c_k|^2 \quad (4)$$

D. Mass distribution image prediction

Mass distribution image of the new subject is predicted by warping the image of another subject based on the differences between two subjects' features (Fig. 4). The technique is called feature-based image warping [3], where source image is transformed into destination image so that features in source image become corresponding features in destination image.

We used 28 features for the warping of mass image (Fig. 3). The 15 mediolateral lines determine segmental width. The 13 longitudinal lines connect the midpoints of mediolateral lines and indicate segmental length.

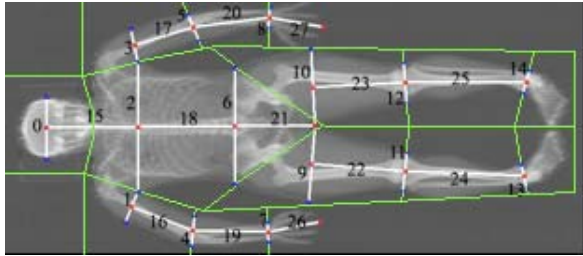


Figure 3: Body composition image produced by Hologic QDR Software together with our defined body segmentation and feature lines. Green lines segment the whole body into 14 parts. White lines are the features required for predicting a new mass image. Mediolateral lines are numbered from 0 to 14, while longitudinal lines are numbered from 15 to 27.

For each mass image prediction, we built a pair of feature lines, one for source image and one for predicted image. Source features were built directly from body composition image and its segmentation (Fig. 3), while destination features were predicted from source features and the relationships between external measurements of source and destination subjects, such as segmental length and girth. It can be done with common assumptions that the cross-sectional area of each body segment was elliptical [12] and the ratio between segmental width and thickness is almost constant for each segment [19]. Hence, the ratio between segmental widths of source and predicted images is almost identical to the ratio between measured segmental girths of source and destination subjects. After mediolateral features were determined, longitudinal features for predicted image were created by connecting the midpoints of mediolateral lines.

In order to obtain a good approximation to destination subject's actual mass distribution, it is important to choose a source subject that resembles destination body type closely. Root-mean-square difference between features length in source and destination subjects was minimized to give a good match in front view. Since mass image does not store depth information, we also compared total body mass divided by sum of squares of features length to avoid significant difference in body thickness of source and destination subjects.

The predicted mass image is subsequently normalized so that predicted whole body mass is equal to the actual mass.

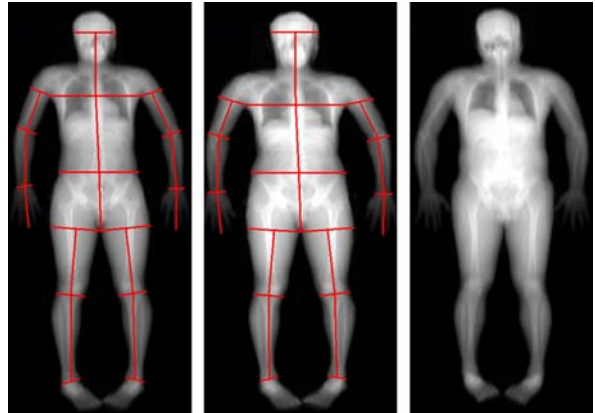


Figure 4: (Left) Mass image and features of a chosen source subject. (Middle) Predicted mass image with new features built from source features and relationships between two subjects' measurements. (Right) New subject's actual mass image.

III. RESULTS

We built a set of mass distribution images from 18 adult male participants with age from 18 to 52, height from 170cm to 182cm and weight from 53kg to 76kg. Feature lines and body segmentation were defined for each image, together with external body measurements and mass.

To evaluate the errors of our method, we estimated BSP for each subject using image-based regression and examined them with values computed directly from DXA, which has been found to be an accurate criterion for 2-D BSP information [7]. The errors were then compared with that in non-linear cadaver-based regression method [19] (Table 1).

	Cadaver-based Regression (%)	Image-based Regression (%)
Head	15	6.9
Torso	15	7.3
Mean	15	7.1
Upper Arm	10	8.1
Lower Arm	11	6.6
Hand	15	9.5
Upper Leg	8	6.2
Lower Leg	5	6.1
Foot	7	8.8
Mean	9.3	7.5

Table 1: Percentage errors for the moments of inertia computed by cadaver-based regression approach [19] and by our image-based regression method.

In image-based method, the mean errors are 7.5% for limbs and 7.1% for head and torso, while the corresponding errors are 9.3% and 15% in cadaver-based method. The differences are significant, especially for head and torso, which contain a large fraction of body mass.

IV. CONCLUSIONS

In this paper, we propose a non-linear image-based regression approach for estimating accurate BSP. Our approach works for all ranges of body types and dimensions since it is not based on cadaveric data. It does not require as many body measurements as in traditional regression methods, and involves much lower radiation level and cost compared to other imaging techniques. Moreover, the accuracy of our method can be easily improved by building a larger database of source images, which is feasible since the subjects are living humans.

One limitation of our approach is the lack of features for small areas such as shoulders and feet, which may lead to errors in those regions. Our approach is currently two-dimensional, due to the lack of depth information in DXA image. It can be extended to three-dimensional by incorporating modeling techniques. An extension to DXA for 3-D reconstruction has also been recently studied [13].

ACKNOWLEDGMENT

The authors wish to thank the Agency for Science, Technology And Research (A*STAR) for funding this research and Physical Education and Sports Science, National Institute of Education for permission to use DXA scanner.

REFERENCES

1. Andrews J G, Mish S P. Methods for investigating the sensitivity of joint resultants to body segment parameter variations. *Journal of Biomechanics* 29, 1996, pp 651-654.
 2. Barter J T. Estimation of the mass of body segments. WADC Technical Report, Wright-Patterson Air Force Base, Ohio, 1957, pp 57-260.
 3. Beier T, Neely S. Feature-Based Image Metamorphosis. *Computer Graphics (SIGGRAPH '92)*, 1992, pp 35-42.
 4. Chandler R F, Clauser C E, McConville J T, Reynolds H M, Young J W. Investigation of inertial properties of the human body. AMRL Technical Report, Wright-Patterson Air Force Base, Ohio, 1975, pp 74-137.
 5. Clauser C E, McConville J T, Young J W. Weight, Volume, and Center of Mass of Segments of the Human Body. Aerospace Medical Research Laboratory, Wright-Patterson Air Force Base, Dayton, OH, Technical Report, 1969, AMRL-TR-69-70.
 6. Dapena J. A method to determine the angular momentum of a human body about three orthogonal axes passing through its center of gravity. *Journal of Biomechanics* 11, 1978, pp 251-256.
 7. Durkin J L, Dowling J J, Andrews D M. The measurement of body segment inertial parameters using dual-energy x-ray absorptiometry. *Journal of Biomechanics* 35, 2002, pp 1575-1580.
 8. Durkin J L, Dowling J J. Analysis of body segment parameter differences between four human populations and the estimation errors of four popular mathematical models. *Journal of Biomechanical Engineering* 125, 2003, pp 515-522.
 9. Hearn D, Baker M P. *Computer Graphics with OpenGL*. Prentice Hall, 2003.
 10. Hinrichs R N. Regression equations to predict segmental moments of inertia from anthropometric measurements: an extension of the data of chandler et al. *Journal of Biomechanics* 18, 1985, pp 621-624.
 11. Huang H K. Evaluation of cross-sectional geometry and mass density distributions of humans and laboratory animals using computerized tomography. *Journal of Biomechanics* 16, 1983, pp 821-832.
 12. Jensen R K. Body segment mass, radius and radius of gyration proportions of children. *Journal of Biomechanics* 19, 1986, pp 359-368.
 13. Le S N, Lee M K, Banu S, Fang A C. Volumetric reconstruction from multi-energy single-view radiography. *Computer Vision and Pattern Recognition*, 2008, pp 1-8.
 14. Martin P E, Mungiole M, Marzke M W, Longhill J M. The use of magnetic resonance imaging for measuring segment inertial properties. *Journal of Biomechanics* 22, 1989, pp 367-376.
 15. Pearsall D J, Raid J G, Livingston L A. Segmental inertial parameters of the human trunk as determined from computed tomography. *Annals of Biomedical Engineering* 24, 1996, pp 198-210.
 16. Pearsall D J, Costigan P A. The effect of segment parameter error on gait analysis results. *GAIT & POSTURE* 9, 1999, pp 173-183.
 17. Press W H, Flannery B P, Teukolsky S A, Vetterling W T. *Cubic Spline Interpolation. Numerical Recipes in FORTRAN: The Art of Scientific Computing*, 2nd edition, 1992, pp 107-110.
 18. Rao G, Amarantini D, Berton E, Favier D. Influence of body segments' parameters estimation models on inverse dynamics. *Journal of Biomechanics* 39, 2006, pp 1531-1536.
 19. Yeadon M, Morlock M. The appropriate use of regression equations for the estimation of segmental inertia parameters. *Journal of Biomechanics* 22, 1989, pp 683-689.
 20. Zatsiorsky V, Seluyanov V. The mass and inertia characteristics of the main segments of the human body. *Biomechanics VIII-B. Human Kinetics Publishers Champaign, IL.*, 1983, pp 1152-1159.
- Author: Le Ngoc Sang
 - Institute: National University of Singapore
 - Street: Computing 1, Law Link, Singapore 117590
 - City: Singapore
 - Country: Singapore
 - Email: lnsang@nus.edu.sg
- Author: Lee Mei Kay
 - Institute: Republic Polytechnic
 - Street: 9 Woodlands Avenue 9, Singapore 738964
 - City: Singapore
 - Country: Singapore
 - Email: lee_mei_kay@rp.sg
- Author: Anthony Fang
 - Institute: National University of Singapore
 - Street: Computing 1, Law Link, Singapore 117590
 - City: Singapore
 - Country: Singapore
 - Email: afang@comp.nus.edu.sg